



THE UNIVERSITY *of* EDINBURGH

Edinburgh Research Explorer

Foliar water uptake in Amazonian trees: evidence and consequences

Citation for published version:

Binks, O, Mencuccini, M, Rowland, L, Da Costa, ACL, De Carvalho, CJR, Bittencourt, P, Eller, C, Sales Teodoro, G, Carvalho, EJM, Soza, A, Ferreira, L, Vasconcelos, SS, Oliveira, R & Meir, P 2019, 'Foliar water uptake in Amazonian trees: evidence and consequences', *Global Change Biology*.
<https://doi.org/10.1111/gcb.14666>

Digital Object Identifier (DOI):

[10.1111/gcb.14666](https://doi.org/10.1111/gcb.14666)

Link:

[Link to publication record in Edinburgh Research Explorer](#)

Document Version:

Peer reviewed version

Published In:

Global Change Biology

General rights

Copyright for the publications made accessible via the Edinburgh Research Explorer is retained by the author(s) and / or other copyright owners and it is a condition of accessing these publications that users recognise and abide by the legal requirements associated with these rights.

Take down policy

The University of Edinburgh has made every reasonable effort to ensure that Edinburgh Research Explorer content complies with UK legislation. If you believe that the public display of this file breaches copyright please contact openaccess@ed.ac.uk providing details, and we will remove access to the work immediately and investigate your claim.



1 Foliar water uptake in Amazonian trees: evidence and consequences

2

3 Oliver Binks¹, Maurizio Mencuccini², Lucy Rowland³, Antonio C.L. da Costa⁴, Claudio José
4 Reis de Carvalho⁵, Paulo Bittencourt³, Cleiton Eller³, Grazielle Sales Teodoro⁶, Eduardo Jorge
5 Maklouf Carvalho⁵, Azul Soza⁷, Leandro Ferreira⁸, Steel Silva Vasconcelos⁵, Rafael Oliveira⁷,
6 Patrick Meir^{1,9}.

7 1. Research School of Biology, The Australian National University, Canberra, 2601 ACT,
8 Australia

9 2. ICREA at CREAF, Barcelona 08010, Spain

10 3. Geography, College of Life and Environmental Sciences, University of Exeter, Amory
11 Building, Exeter, EX4 4RJ, UK

12 4. Centro de Geosciências, Universidade Federal do Pará, Belém 66075-110, Brasil

13 5. EMBRAPA Amazônia Oriental, Belém 66095-903, Brasil

14 6. Biology Institute, Universidade Federal do Pará, Belém, Pará State (66075-110) Brazil

15 7. Department of Plant Biology, Institute of Biology, University of Campinas, Campinas,
16 13.083-970, Brazil

17 8. Museu Paraense Emílio Goeldi, Belém 66077-830, Brazil

18 9. School of Geosciences, University of Edinburgh, Edinburgh EH9 3FF, UK

19 *Corresponding author:* Oliver Binks, Oliver.Binks@anu.edu.au, +612 6125 9037

20 *Key words:* predawn disequilibrium, drought stress, dew, hydraulic vulnerability, tropical
21 rainforest, Amazon, precipitation

22 *Paper type:* Primary research article

23 **Abstract**

24 The absorption of atmospheric water directly into leaves enables plants to alleviate the water
25 stress caused by low soil moisture, hydraulic resistance in the xylem and the effect of gravity on
26 the water column, whilst enabling plants to scavenge small inputs of water from leaf wetting
27 events. By increasing the availability of water, and supplying it from the top of the canopy (in a
28 direction facilitated by gravity), foliar uptake (FU) may be a significant process in determining
29 how forests interact with climate, and could alter our interpretation of current metrics for
30 hydraulic stress and sensitivity. FU has not been reported for lowland tropical rain forests; we
31 test whether FU occurs in six common Amazonian tree genera in lowland Amazônia, and make a
32 first estimation of its contribution to canopy-atmosphere water exchange. We demonstrate that
33 FU occurs in all six genera and that dew-derived water may therefore be used to ‘pay’ for some
34 morning transpiration in the dry season. Using meteorological and canopy wetness data, coupled
35 with empirically-derived estimates of leaf conductance to FU (k_{fu}), we estimate that the
36 contribution by FU to annual transpiration at this site has a median value of 8.2 % (103 mm yr⁻¹)
37 and an interquartile range of 3.4 to 15.3 %, with the biggest sources of uncertainty being k_{fu} and
38 the proportion of time the canopy is wet. Our results indicate that FU is likely to be a common
39 strategy and may have significant implications for the Amazon carbon budget. The process of
40 foliar water uptake may also have a profound impact on the drought tolerance of individual
41 Amazonian trees and tree species, and on the cycling of water and carbon, regionally and
42 globally.

43

44 **Introduction**

45 In the classic scheme of a soil-plant-atmosphere-continuum, water moves from the soil, through
46 the plant, evaporates from the leaf surfaces, and precipitation from atmospheric moisture then
47 replenishes soil water (Tyree *et al.*, 2002). However, where vegetation cover is dense, the water
48 from some leaf-wetting events, such as dew, fog (so-called ‘occult precipitation’) and even light
49 rainfall, is intercepted by foliage and most does not reach the soil. In the classical view, occult
50 precipitation events do not contribute directly to plant water status. However, there is mounting
51 evidence that water uptake by leaves, or foliar uptake (FU), plays a significant role in a wide
52 range of ecosystems. Foliar uptake has been found to occur in desert ecosystems (Nadezhkina &
53 Nadezhdin, 2017, Yan *et al.*, 2015), savanna (Oliveira *et al.*, 2005), the Mediterranean
54 (Fernandez *et al.*, 2014, Gouvra & Grammatikopoulos, 2003), temperate forests (Anderegg *et*
55 *al.*, 2013, Boucher *et al.*, 1995, McDowell *et al.*, 2008, Simonin *et al.*, 2009, Stone, 1957),
56 tropical montane cloud forests (Eller *et al.*, 2013, Goldsmith *et al.*, 2013), and has been reported
57 in conifers (Breshears *et al.*, 2008, Limm *et al.*, 2009), broadleaf trees (Fernandez *et al.*, 2014)
58 and herbaceous vegetation (Gouvra & Grammatikopoulos, 2003), meaning that the large-scale
59 effects and importance of occult precipitation may be greater than previously understood.

60 The occurrence of water entering leaves directly from the atmosphere has two major
61 implications, the first being that it increases the total amount of water available to the plant, and
62 by extension the amount of carbon assimilated (Berry *et al.*, 2014, Oliveira *et al.*, 2014). The
63 second implication is that water entering at the top of the system can effectively act
64 independently of the cohesion-tension theory; that is, it enables water pressure in the canopy
65 xylem to be above the theoretical maximum pressure based on water supply from the soil
66 (Goldsmith, 2013), and hypothetically even achieve positive pressures.

67 A consequence of the first point is that if, in a given system, FU is a common trait and
68 quantitatively important, the representation of carbon-water relationships is likely to be
69 incomplete in models if, as is almost universally the case, the water-supply component is based
70 only on soil water or precipitation. Typically, water intercepted by the canopy is assumed to
71 temporarily depress photosynthesis due to occlusion of stomata and the scattering and reflection
72 of radiation by surface water (Gerlein-Safdi *et al.*, 2018, Pariyar *et al.*, 2017, Rosado & Holder,
73 2013) and, until recently, has not been thought to contribute significantly to the plant water
74 budget (Dawson & Goldsmith, 2018). If, on the other hand, wet leaves become rehydrated,
75 rather than reducing carbon assimilation, the additional water will effectively be offset or
76 reversed enabling the plant to achieve higher stomatal conductance at some later point during the
77 day.

78 The second consequence is more complex. According to the cohesion-tension theory, the
79 evaporation of water from leaves generates tension in the water column, and water moves down
80 a gradient of tension from higher to lower pressure, minus the effects of gravity (Dixon & Joly,
81 1895). Gravity results in a pressure drop in the water column proportional to height, so for flux
82 to occur, the pressure difference must be greater than 0.1 MPa for every 10 vertical meters
83 (Roderick, 2001). Any point above 10 m height in a tree, therefore, is expected to have a water
84 potential (Ψ) lower than -0.1 MPa (a pressure equivalent to absolute vacuum), even if the roots
85 are in a soil that is saturated. Hydraulic systems like tall trees are subject to a number of
86 biophysical limitations, even under such conditions of maximum hydration: 1) upper leaves are
87 always the driest part of the plant and require water to be transported from distant organs below,
88 resulting in negative water potentials associated with resistance of the hydraulic pathway and the
89 height difference between leaves and the storage organ; 2) assuming that woody tissue

Foliar water uptake in Amazonian trees

90 capacitance is similar throughout the plant, the relative water content i.e. stored water, will
91 always be highest in organs most distant from leaves and decrease with proximity to the leaves
92 where the water is required; and 3) low water potentials in the xylem cause conduits to cavitate,
93 causing a reduction in hydraulic conductance which is costly to restore, if restoration is possible.

94 FU modifies these relationships. If water is absorbed directly into the leaves, the water potential
95 can be higher than the theoretical maximum according to the cohesion-tension theory (Kangur *et al.*
96 *al.*, 2017, Simonin *et al.*, 2009). This means that predawn water potential, a common metric for
97 assessing drought stress in plants and soil water potential, does not accurately represent the
98 system (plant and soil) when the leaves have been wet i.e., the leaves could theoretically have a
99 higher tissue water potential, i.e. be ‘wetter’, than the soil. If a fraction of the water lost in
100 transpiration comes from FU, less water is transported from distant organs, reducing the effect of
101 resistance in the hydraulic pathway on the water potential of the leaves. A supply of water direct
102 to the leaves reduces the impact of a loss of conductance in the stem xylem to the leaves and,
103 hypothetically, water taken up by leaves could cause high enough xylem pressures to repair
104 embolised conduits passively (Mayr *et al.*, 2014). These factors may alter the interpretation of
105 existing metrics for assessing drought sensitivity, such as the P50 (Ψ at 50% loss of hydraulic
106 conductance) and the hydraulic safety margin (the difference between a typical and the critical
107 level of drought stress – this is always estimated without accounting for foliar water uptake).

108 An emergent consideration of foliar water uptake is the effect it could have on forest-climate
109 interactions. If forests are gaining small inputs of water from precipitation events such as dew
110 and fog, then this occult precipitation may supply small but essential quantities of water (and
111 therefore carbon) throughout the dry season and other periods of drought stress. Dew formation
112 is very sensitive to temperature and humidity, meaning that small changes in climate may have a

113 large impact on this potentially crucial source of water and, therefore, on forest drought
114 tolerance.

115 Given these considerations, it is important to assess how common foliar water uptake is in forests
116 globally, and the impact of FU on ecosystem functioning. Foliar uptake has been shown to result
117 in improvements in plant water status in multiple biomes (Eller *et al.*, 2013, Gouvra &
118 Grammatikopoulos, 2003, Simonin *et al.*, 2009), but has not been investigated in terms of the
119 quantitative impact it has on ecosystem-level water and carbon exchange. The Amazon accounts
120 for over half of the world's rainforests (Fritz *et al.*, 2003), is considered to be a powerful
121 regulator of the global carbon cycle (Le Quere *et al.*, 2013), and its biophysical functioning is
122 known to be strongly sensitive to reductions in water availability (Gatti *et al.*, 2014, Meir &
123 Woodward, 2010, Phillips *et al.*, 2009). To our knowledge, there are no reports yet addressing
124 the occurrence of foliar water uptake in lowland tropical rain forests, the impact FU might have
125 on large-scale fluxes of carbon and water, and whether or not FU may influence the response of
126 forests to climate change.

127 We tested the central hypothesis that foliar water uptake exists in six hyper-dominant genera (ter
128 Steege *et al.*, 2013) in lowland Amazon rainforest by using a range of both *in situ* and laboratory
129 experiments including wetting experiments, predawn leaf water potentials, and sap flux to assess
130 the occurrence and magnitude of FU at an eastern Amazon rainforest. This multi-method
131 ecophysiological approach was coupled with 15 years of meteorological data and 1 year of
132 canopy-profile leaf wetness data and used to address the following questions: (i) do Amazonian
133 trees take up water directly from the atmospheric environment via their leaves?; and (ii) could
134 water taken up via FU in Amazonian trees make an important contribution to the transpiration

135 budget? We then discuss the implications of foliar uptake in the context of hydraulic
136 vulnerability, carbon exchange and changing climate.

137 **Materials and methods**

138 *Study Site*

139 The study was undertaken in the Caxiuanã National Forest Reserve in the eastern Amazon
140 (1°43'S, 51°27'W). The site is situated in lowland *terra firme* rainforest 10-15 m above river
141 level. The site has a mean temperature of ca. 25 °C, receives 2000 – 2500 mm of rainfall
142 annually and has a dry season in which rainfall is <100 mm per month between June and
143 November. The soil is a yellow oxisol of 3-4 m depth, below which is a narrow laterite layer
144 0.3-0.4 m thick (Fisher *et al.*, 2007, Meir *et al.*, 2015).

145 Meteorological data including temperature, relative humidity (aspirated psychrometer, WP1-
146 UM2, Delta-T Devices, Cambridge, UK) and rainfall (tipping bucket rainfall gauge, Campbell
147 Scientific, Loughborough, UK) have been recorded continuously from the top of a 40 m high
148 above-canopy tower since 2001. Leaf wetness sensors (LWS, Decagon, Labcell Ltd., Four
149 Marks, UK) were used to measure a two full vertical profiles of canopy (leaf) wetness at heights
150 of 10, 20, 25, 30, 32, 34, 36, 38 and 40 m from the ground. The dataset from the leaf wetness
151 sensors is from December 2016 to December 2017.

152 *Study specimens*

153 This study uses mature upper-canopy trees from six genera: *Manilkara*, *Eschweilera*, *Pouteria*,
154 *Protium*, *Swartzia*, and *Licania*. Of the six, *Eschweilera*, *Protium*, *Pouteria* and *Licania* are
155 ranked as the top four most abundant Amazonian genera; *Swartzia* is ranked 17th and *Manilkara*
156 is ranked 73rd (ter Steege *et al.*, 2013). Where possible, a single species was used to represent a

Foliar water uptake in Amazonian trees

157 genus (*Pouteria anomala* (Pires) T.D. Penn., *Manilkara bidentata* (A.DC.) A.Chev., *Swartzia*
158 *racemosa* (Benth.)), but more than one species was used where there were too few individuals in
159 a species over the study area: *Eschweilera* is represented by the species *E. coriacea* (DC.)
160 S.A.Mori, *E. grandiflora* (Aubl.) Sandwith, and *E. pedicellata* (Rich) S.A.Mori, *Licania* by *L.*
161 *membranacea* (Sagot ex Laness) and *L.octandra* (Kuntze) and *Protium* by *P.tenuifolium* Engl.
162 and *P. paniculatum* Engl. Sample leaves and branches were all collected from the upper-canopy
163 where they would have been exposed to full sunlight for at least a proportion of the day.
164 Because of the physical difficulty of sampling, high species diversity and consequent relatively
165 low replication at the genus/species level, data from all trees were grouped for the statistical
166 analyses to give plot-level results.

167 *Experiments*

168 The ingress of water to detached leaves was measured using a series of wetting experiments.
169 The occurrence of FU *in situ* was determined by comparing predawn leaf water potentials with
170 the theoretical maximum leaf water potential (Ψ_{\max}) of all species, and by measuring reverse sap
171 flux in terminal branches of *Manilkara*.

172 *Wetting experiments*

173 *Artificial rainfall experiment*

174 Leaves, collected at midday, were transported from the field into the laboratory in a sealed
175 plastic bag that had been blown into to reduce further water loss. Leaf water potential was taken
176 (Ψ_{initial}) using a Scholander pressure chamber (PMS Instruments Co., Corvallis, OR, USA), after
177 which the open end of the petiole was sealed using cyanoacrylate adhesive ('superglue') to
178 prevent non-lamina water uptake. Leaves were supported in a horizontal position by inserting

Foliar water uptake in Amazonian trees

179 the petiole into a small section of silicon tubing (approximately 20 mm long) which, in turn, was
180 fastened to a freestanding wooden post. ‘Rain’ was created by drilling evenly spaced holes, 0.8
181 mm diameter and 20 mm apart, in the bottom of a bucket. The bucket was supported above the
182 leaves while being continuously supplied with water to generate a constant flow rate. Leaves
183 were subjected to 1 hour of artificial rain from the bucket arrangement, in shaded conditions at
184 ambient temperature (26 – 28 °C). Following the rain event the leaves were immediately patted
185 dry with paper towels and placed in sealed plastic bags. The glued tip of the petiole was
186 removed before measuring the final water potential (Ψ_{final}). Because the data were not normally
187 distributed, and could not be adequately transformed into a normal distribution, paired Wilcoxon
188 signed rank tests were used to test the hypotheses that $\Psi_{\text{initial}} < \Psi_{\text{final}}$ and $\text{mass}_{\text{initial}} < \text{mass}_{\text{final}}$, for
189 significance.

190 *Humidity and condensation experiment*

191 Leaves were collected as in the artificial rainfall experiment, and their water potential and mass
192 were measured before being put into a sealed chamber with over 98% relative humidity. Water
193 potential and mass were taken again after 6 and 19 hours in the chamber. The humidity chamber
194 consisted of a sealed plastic box in which leaves were placed on a mesh between free water (20
195 mm below) and a damp towel (100 mm above). The lid of the box was tightly fitting and was
196 further sealed using thin-film low-density polyethylene (‘cling wrap’) to prevent gas exchange
197 between the internal and external environments. The actual vapour pressure was calculated
198 using the psychrometric equation and the temperature difference between the leaves (dry bulb)
199 and whichever was cooler: the surface of the water or the damp towel (wet bulb), as measured
200 with copper-constantan type T thermocouples connected to a CR1000 data logger (Campbell
201 Scientific, Logan, USA). Leaf temperature was always between the temperature of the water

Foliar water uptake in Amazonian trees

202 surface and the damp towel, therefore creating the possibility of condensation on the leaf surface.
203 As above, differences in water potential and mass before and after treatment were tested for
204 significance using paired Wilcoxon signed rank tests.

205 *Lamina rehydration experiment*

206 To measure the rate of water potential change in response to FU, leaves, collected as above, were
207 measured for water potential and mass before and after being submerged in water (with petioles
208 remaining dry) for periods of three minutes. Following submersion, the leaves were dried with
209 paper towel and allowed to equilibrate in sealed plastic bags for a minimum of five minutes
210 before being remeasured. This was repeated four times on each leaf, on 72 leaves from the six
211 study genera (three leaves per tree, minimum of three trees per genus, except for *Swartzia*, which
212 is represented by only two trees). The nonlinear least squares function was used to test if the
213 relationship between the final leaf water potential and the rehydration time was consistent with
214 the equation describing the recharging of a capacitor (Brodribb & Holbrook, 2003).

215 In situ FU measurement

216 *Leaf water potentials*

217 Leaf water potentials were taken from branches collected from the top of the canopy between
218 05:30 and 07:00 (Ψ_{predawn}) and 12.00 and 14.00 (Ψ_{midday}). These measurements were made in
219 October 2013, June 2014, October and November 2015, June 2016 and December 2016, where
220 June is the end of the wet season and October to December is the end of the dry season. Water
221 potential was taken on three leaves per tree (exceptionally two leaves per tree), and on three trees
222 per genus per field campaign.

Foliar water uptake in Amazonian trees

223 For the measurements taken in December 2016, the height of the sampled leaves was also
224 measured using a Suunto Optical Reading Clinometer (Suunto, Sweden). The measured water
225 potential values were compared with the theoretical maximum (least negative) water potential
226 (Ψ_{t_max}) at the given height and soil water potential (Ψ_{soil}) as per the relationship: $\Psi_{t_max} = \Psi_{soil} -$
227 ρgh where ρ is the density of water, g is gravity, and h is the height of the sample. Because a
228 genus-level separation was noticed in the relationship between $\Psi_{predawn}$ and height, a general
229 linear model was used to test for a statistically significant difference between genera.

230 For $\Psi_{predawn}$ measurements taken prior to 2016, precise height measurements were not available
231 for the sampled branches. To make sure we did not underestimate the Ψ_{t_max} (i.e., too negative,
232 and hence overestimate the observed water potential disequilibrium at predawn), we assumed
233 that branches were sampled at 15 m height which was the minimum height of any predawn water
234 potential leaf sample. This provided a conservative estimate of the effect of height on leaf water
235 potential.

236 *Soil water potential, Ψ_{soil}*

237 Volumetric soil water content ($m^3 m^{-3}$) was measured at depths of 0, 0.5, 1 and 2.5 m using
238 CS616 soil moisture sensors (Campbell Scientific, Logan, USA) in one soil pit and converted to
239 Ψ_{soil} using the widely-applied Van Genuchten (1980) model:

$$240 \quad \Psi_{soil} = \frac{\left(\left[\frac{\theta - \theta_r}{\theta_s - \theta_r} \right]^{-n/n-1} - 1 \right)^{1/n}}{\alpha}$$

241 where θ is volumetric water content, θ_r residual water content, θ_s saturated water content, n is a
242 scaling factor which determines the curve shape, and α is a value proportional to the maximum
243 pore size (kPa^{-1}). A pressure plate analysis was performed on four soil samples taken from each

244 depth, from the same pit in which the water content sensors were installed, measuring θ at
245 pressures of 0, 6, 10, 30, 100, 500 and 1500 kPa, where the θ at 0 kPa = θ_s (Richards & Fireman,
246 1943). The residual water content, θ_r , is taken to be the point at which the gradient of the slope
247 between θ and pressure tends to 0. Here, it was taken to be the θ at which there was < 0.1 %
248 change over 10 MPa difference in pressure. The parameters α and n were fitted using a non-
249 linear least squares regression (Fig S1.1).

250 The soil water content sensors occasionally measured θ values < θ_r , posing a limitation on the
251 model i.e. the model cannot function using negative percent saturation values. Moreover, an
252 inflection point in the relationship between Ψ_{soil} and θ means that θ values close to θ_r generate
253 excessively low water potentials e.g. < -100 MPa. We speculate that this is a limitation of using
254 the van Genuchten model to derive water potential at such low water content given the precision
255 of the sensors (+/- 2.5 % volumetric water content). Given this limitation, $\Psi_{\text{soil}} < -5$ MPa were
256 excluded from the results, using instead a mean value from the other soil layers, which resulted
257 in a more conservative outcome with respect to the analysis. The soil water potential
258 measurements are listed in Table S1 together with the measurement periods and depths that were
259 out of range.

260 A mean Ψ_{soil} of all soil depths, from 0 to 2.5 m, which should account for > 99.9 % of
261 cumulative root fraction (Galbraith, 2010, Jackson *et al.*, 1996), was used to represent soil water
262 potential for the purpose of calculating the maximum theoretical predawn leaf water potential.
263 Soil moisture values intermittently fell outside the limit of calculation, as described above, thus
264 not all mean Ψ_{soil} values have the same n . As there was no systematic failure of sensors at a
265 particular depth, this was not thought to bias the soil water potential values.

266 *Sap flux*

267 Upper-canopy measurements of sap flux were limited by access and were made on two terminal
268 branches of a single *Manilkara bidentata* tree that was fully accessible from a canopy tower.
269 Because of the low replication of the sap flux data, these results are provided as auxiliary data in
270 support of the findings of the other lines of evidence, although the data are not fundamental to
271 the conclusions of the study. In 2015, sap flux sensors (ICT International, Armadale, Australia)
272 were installed in two places on one branch, first at a position measuring 17.2 mm in diameter and
273 then further upstream at 50.8 mm in diameter. In 2016, sensors were installed in another branch
274 of the same tree <20 mm in diameter. Because the sensor probes (35 mm long) extended through
275 the branches, blocks of closed-cell foam were used to insulate the exposed ends and the probes
276 and branch segment were wrapped in aluminium foil to reduce the potential for radiative heating
277 of the probes. Sap flux was measured for a period of seven days during the dry seasons of 2015
278 and 2016 and the branches were then removed to get an unequivocal zero value for sap flow.
279 Sap flow velocity was calculated according to Burgess et al. (2001).

280 *Leaf conductance to the uptake of surface water, k_{fu}*

281 Here we treat k_{fu} as a purely physical process in which the flux, F , into the leaf is proportional to
282 the water potential gradient between the surface water on the leaf, Ψ_{surface} , and the water potential
283 in the leaf, Ψ_{inside} , such that $k_{fu} = F / (\Psi_{\text{surface}} - \Psi_{\text{inside}})$ consistent with Ohm's Law (Sack &
284 Holbrook, 2006). Therefore, using a modified form of the equation that describes discharge of
285 a capacitor, k_{fu} can be determined thus: $k_{fu} = -C \ln[\Psi_{\text{initial}}/\Psi_{\text{final}}] / t$, where C is hydraulic
286 capacitance (mol MPa^{-1}), Ψ_{initial} and Ψ_{final} are the water potentials before and after wetting
287 respectively, and t is duration of wetting (Brodribb & Holbrook, 2003). k_{fu} was calculated using
288 the change in water potential ($\Delta\Psi$) and time (t) from the lamina rehydration experiment, and the
289 leaf capacitance derived from pressure volume curves (Binks *et al.*, 2016).

Foliar water uptake in Amazonian trees

290 We also used an alternative method of deriving k_{fu} using the mean value of 6 nights' reverse sap
291 flux (V , g hr⁻¹) that occurred at 06:00 hrs, normalised by the leaf area of the branch (A_f) and
292 predawn leaf water potential ($\Psi_{predawn}$): $K_{fu_sf} = V / [A_f \Psi_{pd}]$.

293 The sap flux-derived term for k_{fu} is an underestimate because it does not take into account the
294 storage of water between the leaves and the sensors and its calculation also assumes 100 % leaf
295 wetness. Moreover, it is based only on the uptake by one species. For those reasons, the
296 capacitance-derived term was used in the model of canopy-scale water uptake.

297 In this study, k_{fu} does not distinguish between the conductances of the abaxial and adaxial
298 surfaces, and represents water taken up by the whole leaf surface area (e.g., both sides as per
299 Guzman-Delgado et al. (2018)). See SI section 'S2. Determining leaf hydraulic conductance to
300 foliar water uptake' for a detailed explanation of the determination of k_{fu} .

301 *Calculating canopy foliar water uptake (U_c)*

302 The total annual water uptake of the canopy U_c (g H₂O m⁻² ground area yr⁻¹) is calculated by the
303 relationship

$$304 \quad U_c = k_{fu} (\Psi_{surface} - \Psi_{canopy}) P_p L t_y$$

305 where k_{fu} is the conductance of the leaf cuticle to water (g MPa⁻¹ s⁻¹ m⁻²), Ψ_{canopy} and $\Psi_{surface}$ are
306 the mean water potential of the canopy and of the surface water (assumed to be 0, i.e. to have
307 negligible solute concentration), respectively (MPa). P_p is the product of the proportion of leaf
308 area index L (m²_{leaf_area} m⁻²_{ground_area}) that is wet, and the proportion of the year that it is wet, as
309 determined by the data from two through-canopy vertical profiles of leaf wetness sensors, and t_y
310 (s yr⁻¹) is the number of seconds in a year. Because this is the first time that canopy-scale foliar
311 water uptake has been calculated, there is inevitably some uncertainty in the true value of the

312 parameters. To account for this, we use simulated data based on empirically-derived
313 distributions of the parameter values to provide a statistical distribution of results. Hence, the
314 output of the model is a distribution based on 10,000 iterations of the equation above using data
315 which have been randomly generated to represent the measured parameter distributions
316 explained below and in Table 1. See SI section ‘S3. *Canopy foliar uptake model parameters*’ for
317 a more detailed explanation of model parameter selection.

318 The distribution of canopy water potential, Ψ_{canopy} , was based on the range of predawn and
319 midday water potentials measured in the wet and dry season (Fig S3.1). The mean wet season
320 water potential (predawn and midday combined) was -0.66 MPa, and the mean dry season water
321 potential was -1.11 MPa. In both seasons, the range between predawn and midday was around 1
322 MPa and, therefore, we used a mid-value of -0.89 MPa and a standard deviation (SD) of 0.5 to
323 generate the distribution of canopy water potentials. This gave maximum and minimum values
324 of 0 and -2.9 MPa respectively, thus accounting for a wide distribution of water potentials
325 spatially (throughout the canopy) and temporally. Initially, estimates of Ψ_{leaf} were made
326 temporally explicit by taking into account diurnal and seasonal fluctuations of Ψ . However, this
327 made little difference to the model and so the simpler method was used. See SI section S3b. *Leaf*
328 *water potential* for a detailed explanation of the temporally explicit leaf water potential
329 calculation.

330 The cumulative duration of leaf wetness over a given time period is $P_p = D_d + D_r + N\bar{D}_e$, where
331 D_d is the duration of dew events, D_r the duration of precipitation events, N the number of
332 precipitation events, and \bar{D}_e is the mean length of time for canopy drying following a rain event.
333 The leaf wetness sensors give a continuous millivolt output in response to surface wetness and
334 typically a clearly defined threshold is selected in which the sensor is either wet or dry

335 (Aparecido *et al.*, 2016). While the magnitude of the sensor output is a poor indicator of how
336 wet the sensor is, dew events have a distinctive signal, characterised by a gradual increase in
337 wetness overnight and abrupt drying at sunrise, which is easy to identify (Fig. S3.2). We used a
338 script, in R, to identify rain events and dew events separately, based on their different signals.

339 Over the course of a year, the leaf wetness sensors detected 141 dew events which occurred on
340 rainless nights, with a mean duration of 3.06 hrs. Thus, 3 hrs of dew were assumed to occur
341 every rainless night in the dry season over the duration of the meteorological dataset from 2001
342 to 2015. The canopy drying time, in response to a rain event, was derived from the leaf wetness
343 sensor drying time. The difference between the sum of the duration of rainfall and dew events
344 ($D_d + D_r$) and the duration of surface wetness of the sensors (D_{lws}) gives the total drying time of
345 the sensors. Thus, the mean sensor drying time is given by $(D_{lws} - D_d - D_r) / N$, where N is the
346 total number of precipitation events.

347 We suspected that the angle of the leaf wetness sensors would influence their drying time and
348 did a further analysis to assess this affect. See SI 'S3 d. Sensor drying time versus leaf drying
349 time' for description of sensor analysis and derivation of correction factor, Fig. S3.3. In order to
350 obtain a closer approximation of canopy drying time from the sensors we applied a correction to
351 the sensor angle of 40° to represent the mean leaf angle in the canopy (Bailey & Mahaffee,
352 2017, Kull *et al.*, 1999, Pisek *et al.*, 2013, Raabe *et al.*, 2015).

353 All statistical analyses were performed in R (R Core Team, 2015).

354 **Results**

355 *Wetting experiments*

Foliar water uptake in Amazonian trees

356 Water taken up through leaves in a 1 hr artificial rainfall experiment significantly increased leaf
357 water potential, Ψ_{leaf} , across all trees, from -1.31 ± 0.06 to -0.68 ± 0.04 MPa, (mean plus or
358 minus standard error, $P < 0.001$, $n = 110$ leaves, minimum 14 leaves per genus, Fig. 1). The
359 mass did not increase significantly in the rainfall experiment ($P = 0.18$), but this test was
360 confounded by fragments of superglue breaking off the petioles while detaching the leaves from
361 the silicon tubes. Leaves placed in an environment of $> 98\%$ relative humidity for 16 hrs
362 significantly increased water potential in all genera ($P < 0.001$, $n = 102$ leaves, minimum 15
363 leaves per genus), with *Eschweilera* having the greatest change and *Licania* the smallest,
364 although there were no significant differences among genera (Fig. S4.1). Fresh mass per area
365 also increased significantly in the humidity experiment ($P < 0.001$, Fig. S4.2). In both the
366 artificial rainfall and humidity experiment there was a strong negative relationship between the
367 change in Ψ ($\Psi_{\text{final}} - \Psi_{\text{initial}}$) and Ψ_{initial} as determined by a linear regression ($R^2 = 0.59$ and 0.69
368 respectively, Fig. 2).

369 The lamina rehydration experiment showed that Ψ_{leaf} increased with each successive wetting
370 event according to the relationship $\Psi_{\text{leaf}} = \Psi_{\text{initial}} e^{-t K/C}$ (voltage capacitance equation), where
371 Ψ_{initial} is Ψ_{leaf} before wetting, t is the duration of wetting, K is k_{fu} , and C is the hydraulic
372 capacitance (Fig. 3). The relationship was significant at $P < 0.001$. See SI section ‘S5. Rate
373 dependence of $d\Psi$ on Ψ_{initial} ’ for an explanation of the relevance of $d\Psi / \Psi_{\text{initial}}$ to k_{fu} . The results
374 from the rainfall, humidity and lamina rehydration experiments all support the known analogue
375 of leaf water uptake and the recharging of a capacitor (Brodrribb & Holbrook, 2003).

376 *Predawn water potentials and leaf height*

Foliar water uptake in Amazonian trees

377 Leaf predawn water potentials (Ψ_{predawn}) conducted in December 2016 revealed a divide between
378 a group of genera that tended have higher Ψ_{predawn} than the theoretical maximum Ψ_{t_max}
379 (*Eschweilera*, *Licania* and *Swartzia*, Fig. 4) and a second group that had higher Ψ_{predawn} than
380 Ψ_{t_max} based on soil water potential only (*Manilkara*, *Pouteria* and *Protium*), however the genus-
381 level replication was insufficient to test this relationship for significance. The mean soil water
382 potential (Ψ_{soil}) of depths 0.5 and 1 m was -2.19 MPa over the duration of the Ψ_{predawn} and height
383 measurements (depths 0 and 2.5 were out of the calculable range of water potential during these
384 measurements, Table S1).

385 Of the predawn water potential measurements taken from 2013 to 2016: (i) 25 out of 99 were
386 higher than Ψ_{t_max} taking into account height alone, i.e., assuming $\Psi_{\text{soil}} = 0$ MPa (Fig. 5); (ii) 73
387 out of 86 measurements were higher than the soil, i.e., the leaves were wetter than the soil (Fig.
388 6); and (iii) 80 out of 86 were higher than the Ψ_{t_max} , assuming the combined effect of the
389 minimum leaf sample height of 15 m and the mean soil water potential over the measurement
390 period. The value of $\Psi_{\text{predawn}} - \Psi_{\text{soil}}$ of the dry season data was 1.86 +/- 0.11 MPa standard error,
391 while the wet season was 0.29 +/- 0.05 MPa.

392 *Sap flux*

393 The sap flux data from both of the terminal branches (in 2015 and 2016) revealed that reverse
394 sap flow occurred in *Manilkara bidentata* every night during the dry season in response to the
395 deposition of dew, and rainfall that occurred on two of the eight nights in 2016 (Fig. S4.3 and
396 S4.4). Installing two sensors at different positions on the same branch (performed in 2015)
397 showed that negative flow occurred at a branch position measuring 17.2 mm in diameter, but not
398 at a point more distal from the leaves with a 50.8 mm diameter. This indicated that the water
399 taken up via the leaves was contributing to refilling the hydraulic capacitance of the terminal

Foliar water uptake in Amazonian trees

400 portion of the branches in this species (Fig. S4.3). The duration of measured nocturnal water
401 uptake was typically around seven hours per night; however, the duration of dew deposition
402 tended to be less than that, at around 3 to 4 hours. The disparity in results could be caused by
403 dew forming on the leaves before detectable changes in sensor readings (possibly because of
404 different rates of radiative cooling), or by the uptake of water vapour through open stomata prior
405 to dew point. Data from both terminal branches demonstrate that the maximum rate of reverse
406 sap flux tended to occur at around 06:00 hrs, just before dawn.

407 The cumulative amount of water taken up by the branch, which had a leaf area of 0.66 m²,
408 ranged from 2.3 to 12.0 g over the 8 nights of measurement in 2016, with a mean of 4.9 g +/- 1.0
409 standard error (Fig. S4.4). On one of the nights >55 mm of rain fell between 20:00 and 21:00
410 and over the course of the whole night the total amount of water taken up by the branch was 12.6
411 g, or 19.1 g per m⁻² one-sided leaf area. The water taken up accounted for between 45 and 120
412 minutes of early morning transpiration, as determined from the time interval between the
413 transition from negative to positive sap flux (Fig. 4.4) to the point where the water gained
414 equalled water transpired.

415 *Leaf conductance to foliar water uptake, k_{fu}*

416 The mean +/- standard error k_{fu} for all genera, derived from the lamina rehydration experiment,
417 was 2.24 +/- 0.28 mg m⁻² s⁻¹ MPa⁻¹ (Fig. S2.1), which is of a similar magnitude to the values
418 reported by Guzman-Delgado et al. (2018): 1.5 mg m⁻² s⁻¹ MPa⁻¹ in *Prunus dulcis*, and 0.38 mg
419 m⁻² s⁻¹ MPa⁻¹ in *Quercus lobata*.

420 *Canopy foliar water uptake*

Foliar water uptake in Amazonian trees

421 The median value for yearly canopy-scale foliar water uptake was $102.85 \text{ mm yr}^{-1}$ with an
422 interquartile range (IR) of 43.01 to $191.69 \text{ mm yr}^{-1}$ (Fig. 7). This corresponds to a median
423 contribution of 8.2% of the annual transpiration budget with an IR of 3.4 to 15.3% . Using the
424 data from Fisher et al. (2007) on transpiration (E) and the value for gross primary productivity
425 (GPP), from the same site, a plot-level value of water use efficiency (WUE) was calculated
426 ($\text{GPP}/\text{E} = \text{WUE}$) in order to estimate a site-based carbon-gain value consistent with the amount
427 of extra water taken up via FU at canopy scale. The median value for FU-dependent carbon
428 uptake was $2.5 \text{ t ha}^{-1} \text{ yr}^{-1}$ ($\sim 8\%$ of GPP) with an IR of 1.1 to $4.7 \text{ t ha}^{-1} \text{ yr}^{-1}$ ($\sim 4\text{-}16\%$ of GPP).

429

430 Discussion

431 The results from the multiple experiments presented here consistently demonstrate that foliar
432 water uptake (FU) occurred in all six hyper-dominant genera that were studied, and provide the
433 first evidence that FU may be a common strategy among the dominant tree species of
434 Amazonian rainforests. Combining these multi-taxa leaf hydraulics data from two years of wet
435 and dry seasons with 14 years of meteorological data, and 1 full year of canopy profile leaf
436 wetness measurements we estimate that the total FU-related water uptake by the canopy could
437 account for a median value of 8.2% (103 mm yr^{-1}) of annual transpiration and a potential
438 contingent carbon assimilation of $2.5 \text{ t ha}^{-1} \text{ yr}^{-1}$ ($\sim 8\%$ of GPP).

439 There are many uncertainties regarding how FU affects stand scale carbon and water dynamics,
440 but in our simple model we offer a first estimate of what may be a globally significant flux. The
441 impact of FU will vary depending on climatic conditions. It seems likely that in some years,
442 conditions that favour dew formation in the dry season, e.g., comparatively high humidity and
443 large diurnal temperature changes, will result in a substantial input of FU water together with a

444 contingent carbon flux, and in other years perhaps the quantitative role of FU will be negligible.
445 However, we will not be able to make a better-constrained assessment of this impact until we
446 have an improved understanding of the relevant variables.

447 *Significance and limitations of predawn WP measurements*

448 Our data also demonstrate that predawn water potential in these species routinely overestimates
449 the water status of the soil and particularly in the dry season (Fig. 4, 5, and 6). Measuring the
450 soil water potential that plants are experiencing is challenging because of the uncertainty about
451 rooting depth, and this uncertainty extends to the maximum theoretical water potential (Ψ_{t_max}) of
452 the leaves. Our measurements of soil water content integrate the depths 0 to 2.5 m which should
453 account for 99.99 % of the cumulative root fraction (Galbraith, Jackson *et al.*, 1996). However,
454 this does not rule out the possibility that very deep roots are accessing wetter soil layers.
455 Nevertheless, our analysis shows that even if the soil were saturated, i.e., $\Psi_{soil} = 0$ MPa, many of
456 the predawn water potential values are still above the maximum theoretical value due to height
457 alone (Fig. 4 and 5). Therefore, the results unambiguously demonstrate that foliar uptake
458 elevates leaf water status above the highest value that could be achieved from the uptake of soil
459 water alone in these Amazonian tree species. Assuming that our analysis of soil water potential
460 represents plant-available water, then our results show that the effect of FU is far more
461 substantial in the dry season (Fig. 6), meaning that small quantities of water moving directly into
462 the leaves at regular intervals (often daily from dew) may sustain large upper-canopy trees
463 throughout periods of low water availability. Calculations of the upper limit of leaf water
464 potential can thus be modified to $\Psi_{t_max} = \Psi_{soil} - \rho gh + \Delta\Psi_{FU}$, where $\Delta\Psi_{FU} = dt F_{FU} / C_{leaf}$, and
465 F_{FU} is the flux into the leaf via FU; dt is the duration over which the flux occurs and C_{leaf} is the
466 hydraulic capacitance of the leaf. This equation relates to the relationship set out in Simonin et

467 al. (2009) describing a modified version of the soil-plant-atmosphere-continuum model which
468 includes parameters for foliar water uptake.

469 *The relevance of foliar uptake to drought sensitivity*

470 The transpiration of water stored in the terminal branches (as observed in the sap flux data Fig
471 S4.3 – 4.5) suggests a partial decoupling of canopy processes from soil water and functional
472 stem xylem. This increases the potential for hydraulic recovery following drought periods, and
473 suggests that hydraulic capacitance and water storage in the canopy could be fundamental traits
474 in determining the ability of these species to cope with drought conditions. Furthermore, we
475 suggest that our data change how predawn water potential measurements should be understood.
476 Predawn leaf water potentials are not representative of whole-plant water stress, or soil water
477 potential in these species (Fig. 4, 5 and 6), as tissue water potential is also determined by the
478 duration of leaf wetness, lamina conductance to water (k_{fu}), the hydraulic conductance upstream
479 of the leaf, and the capacitance and water storage of the rest of the plant.

480 The extent to which FU is purely a physical process, of water moving through a permeable
481 barrier down a water potential gradient, versus being a trait which has been subject to selection
482 pressure and thus given rise to physiological adaptations, is poorly understood. If the value of
483 FU is as important as this study suggests it might be, then one would expect adaptations that
484 increase the duration of leaf wetness, e.g., leaf surface morphology, or increase the rate at which
485 water is taken up. The exact route by which water moves into the leaves of these genera is
486 unknown, but studies on non-rainforest taxa have shown water uptake via trichomes (Fernandez
487 *et al.*, 2014, Nguyen *et al.*, 2016), stomata (Burkhardt *et al.*, 2012, Eichert & Goldbach, 2008),
488 directly through the cuticle (Eller *et al.*, 2013), and even adsorption onto the cuticle (Chamel *et*
489 *al.*, 1991, Schönherr & Schmidt, 1979). Of the six genera in this study, only *Licania* has

490 trichomes (on the abaxial leaf surface), suggesting that, instead, the cuticular pathway may be a
491 more common means of water ingress amongst Amazonian taxa. This raises the possibility of a
492 trade-off between traits favouring foliar water uptake and water loss, i.e. cuticular transpiration,
493 due to cuticle permeability. If this trade-off exists, then future increases in vapour pressure
494 deficit (VPD) may lead to a disproportionate rise in hydraulic vulnerability, because of both the
495 loss of water inputs and the increase in water loss. Thus, whether or not the capacity for foliar
496 uptake results in greater cuticular transpiration is a question of pressing importance in evaluating
497 the sensitivity of Amazonian species to predicted future climates.

498 *The potential impact of foliar uptake on carbon balance*

499 The gross primary productivity at this site was calculated to be $30.94 \text{ t C ha}^{-1} \text{ yr}^{-1}$ (Fisher *et al.*,
500 2007). Thus, our median estimate of the possible contribution of FU to carbon gain, 2.5 t C ha^{-1}
501 yr^{-1} equates to over 8 % of the gross primary productivity. This value is based on the potential
502 photosynthesis afforded by the direct uptake of atmospheric water by leaves from all
503 precipitation events throughout the year. However, we also found that dew could ‘pay’ for the
504 first hour of transpiration (Fig S4.5), and this source of water, and its effects, are currently
505 unaccounted for in the classical view of plant-atmosphere interactions. Whilst clearly a first
506 estimate with a quantified but relatively wide uncertainty range, the potential impact of FU on
507 water and carbon cycling in this region suggests the need for detailed further study of the effects
508 of FU in lowland tropical rainforest.

509 Additionally, there may be indirect effects of FU on stand dynamics and ecosystem carbon
510 storage due to the potential influence of FU on drought-induced tree mortality. Because the rate
511 of FU is inversely proportional to leaf water potential (a more negative leaf water potential
512 drives a higher flux), the gradient for water uptake increases in response to drought. This might

513 mean that small precipitation events in the dry season, e.g. dew, are disproportionately important,
514 ecophysiologicaly resulting in greater water uptake at a time that it is most needed. Indeed, this
515 phenomenon may account for the surprisingly small hydraulic safety margin of many tree
516 species globally (Choat *et al.*, 2012). Some of the modelled projections of future Amazonian
517 climate predict increases in dry season length and strengthening of the seasonal cycle (Boisier *et*
518 *al.*, 2015, Fu *et al.*, 2013, Jupp *et al.*, 2010), which could conceivably result in fewer minor
519 precipitation events throughout the dry season. Moreover, higher temperatures are expected to
520 cause elevated VPD in the future (Scheff & Frierson, 2014, Sherwood & Fu, 2014), reducing
521 the likely frequency of dew formation. If many abundant forest tree species are dependent on
522 small precipitation inputs for maintaining favourable water status and avoiding mortal hydraulic
523 risk, such climate scenarios of reduced precipitation and high VPD could increase overall tree
524 mortality risk purely through their impacts on FU-derived leaf water, with consequences for net
525 carbon uptake and storage at large scale.

526 *How can we more accurately quantify the contribution of FU to the forest water budget?*

527 There are a number of challenges associated with getting accurate values of water uptake at the
528 ecosystem-scale. Principally, these are obtaining a reliable mean for canopy k_{fu} , determining
529 what proportion of the canopy is wet, and for how long. Relatively little is known about k_{fu} but it
530 is likely to vary by canopy position, leaf side (Fernandez *et al.*, 2014), and species (Fig. S2.1
531 Eller *et al.*, 2016, Limm *et al.*, 2009). Canopy wetness has the potential to influence large-scale
532 water uptake substantially because of the magnitude of variation over time and space. The study
533 forest here, at Caxiuanã National Forest in the eastern Amazon has a leaf area index of
534 approximately $5.5 \text{ m}^2 \text{ m}^{-2}$ (Fisher *et al.*, 2007) resulting in a maximum absorptive surface of 11
535 m^2 for every m^2 of ground surface if uptake occurs from both sides of the leaf, which may (Eller

536 *et al.*, 2013) or may not (Fernandez *et al.*, 2014) be the case. These two factors might interact
537 such that leaves that are wet for longer have higher rates of foliar uptake. Accordingly, future
538 work must focus on quantifying these parameters.

539 The model we present lacks a feedback term. In reality, as the plant/canopy reaches saturation,
540 the flux will decline. The factors that influence the rate of decline/saturation are the same that
541 influence predawn water potential, namely, the hydraulic conductance of each part of the
542 pathway, the capacitance and water storage capacity of the plant. Theoretically, if the
543 conductance of the water away from the leaf is considerably higher than the conductance into the
544 leaf, k_{fu} , and the capacitance is high, then the outcome will be something similar to our model.
545 However, these parameters, particularly in the context of foliar uptake, and in tropical rain
546 forests, are poorly known, so warrant further investigation.

547 Tropical rainforests present the additional challenge of high species diversity. Here we measured
548 upper canopy trees as these account for a very high proportion of the total forest biomass and
549 transpiration (Brum *et al.*, 2018). However, canopy wetness and k_{fu} may differ throughout the
550 profile of the forest, and among species. In this study, we measured species from six different
551 hyper-dominant genera, but unavoidable low species-level replication prevented us from
552 accurately testing for inter-specific differences. In order to obtain a better-constrained value for
553 the ecosystem-level impact of FU, the variance in FU across the forest, between individuals,
554 species and canopy positions, must be quantified. The results of this study demonstrate that
555 foliar water uptake is likely to be a common strategy across the Amazon, partially decoupling
556 leaves from soil water conditions and allowing canopy water potential to be higher than is
557 considered in classical and current soil-plant-atmosphere computational schemes. Our best
558 estimates based on results from multiple independent measurement approaches suggest that

Foliar water uptake in Amazonian trees

559 water taken up directly into leaves may account for approximately 8 % of annual transpiration,
560 with upper values potentially reaching 15 % (a value comparable to branch-level measurements
561 by Gotsch et al. (2014)). Further, the uptake of dew during periods of substantial water shortage
562 may be a critical mechanism allowing the trees to avoid potentially lethal hydraulic stress, and to
563 maintain small but reliable supplies of water and carbon in the dry season. The carbon
564 assimilation that is attributable to foliar water uptake is uncertain, but our first estimates suggest
565 a range of 1.1 to 4.7 t C ha⁻¹ yr⁻¹ at our study site (4-16% of GPP). This could amount to a
566 significant flux at the scale of the Amazon region which is potentially very sensitive to future
567 changes in temperature and humidity. Foliar uptake of water may thus have a profound impact
568 on the water and carbon cycles at small and large scales, and on the functioning and survival of
569 Amazonian forest trees under future climate change.

570 **Acknowledgments**

571 This work was a product of a UK Natural Environment Research Council PhD studentship tied
572 to grant NE/J011002/1 to P.M. and M.M. P.M. and O.B. also gratefully acknowledge support
573 from ARC FT110100457 and DP170104091, the CNPQ grant 457914/2013-
574 0/MCTI/CNPq/FNDCT/LBA/ESE- CAFLOR to ACLD, the EU FP7 Research Consortium
575 ‘Amazalert’, and the Museu Paraense Emílio Goeldi. P.B, A.S. and R.O. gratefully acknowledge
576 support from Newton International Fellowship (grant NF170370). This study was financed in
577 part by the Coordenação de Aperfeiçoamento de Pessoal de Nível Superior – Brasil (CAPES) –
578 Finance Code 001.

579

580

581

582 **References**

- 583 Anderegg LDL, Anderegg WRL, Berry JA (2013) Not all droughts are created equal: translating
584 meteorological drought into woody plant mortality. *Tree Physiology*.
- 585 Aparecido LMT, Miller GR, Cahill AT, Moore GW (2016) Comparison of tree transpiration
586 under wet and dry canopy conditions in a Costa Rican premontane tropical forest.
587 *Hydrological Processes*, **30**, 5000-5011.
- 588 Bailey BN, Mahaffee WF (2017) Rapid measurement of the three-dimensional distribution of
589 leaf orientation and the leaf angle probability density function using terrestrial LiDAR
590 scanning. *Remote Sensing of Environment*, **194**, 63-76.
- 591 Berry ZC, White JC, Smith WK (2014) Foliar uptake, carbon fluxes and water status are affected
592 by the timing of daily fog in saplings from a threatened cloud forest. *Tree physiology*, **34**,
593 459-470.
- 594 Binks O, Meir P, Rowland L *et al.* (2016) Plasticity in leaf-level water relations of tropical
595 rainforest trees in response to experimental drought. *New Phytologist*, **211**, 477-488.
- 596 Boisier JP, Ciais P, Ducharne A, Guimberteau M (2015) Projected strengthening of Amazonian
597 dry season by constrained climate model simulations. *Nature Climate Change*, **5**, 656-
598 661.
- 599 Boucher JF, Munson AD, Bernier PY (1995) Foliar absorption of dew influences shoot water
600 potential and root-growth in *Pinus-strobus* seedlings. *Tree physiology*, **15**, 819-823.
- 601 Breshears DD, McDowell NG, Goddard KL, Dayem KE, Martens SN, Meyer CW, Brown KM
602 (2008) Foliar absorption of intercepted rainfall improves woody plant water status most
603 during drought. *Ecology*, **89**, 41-47.
- 604 Brodribb TJ, Holbrook MN (2003) Stomatal Closure during Leaf Dehydration, Correlation with
605 Other Leaf Physiological Traits. *Plant Physiology*, **132**, 2166-2173.
- 606 Brum M, Gutierrez Lopez J, Asbjornsen H, Licata J, Pypker T, Sanchez G, Oiveira RS (2018)
607 ENSO effects on the transpiration of eastern Amazon trees. *Philos Trans R Soc Lond B*
608 *Biol Sci*, **373**.
- 609 Burgess SSO, Adams MA, Turner NC, Beverly CR, Ong CK, Khan AaH, Bleby TM (2001) An
610 improved heat pulse method to measure low and reverse rates of sap flow in woody
611 plants†. *Tree physiology*, **21**, 589-598.
- 612 Burkhardt J, Basi S, Pariyar S, Hunsche M (2012) Stomatal penetration by aqueous solutions –
613 an update involving leaf surface particles. *New Phytologist*, **196**, 774-787.
- 614 Chamel A, Pineri M, Escoubes M (1991) Quantitative determination of water sorption by plant
615 cuticles. *Plant, Cell & Environment*, **14**, 87-95.
- 616 Choat B, Jansen S, Brodribb TJ *et al.* (2012) Global convergence in the vulnerability of forests to
617 drought. *Nature*, **491**, 752-+.
- 618 Dawson TE, Goldsmith GR (2018) The value of wet leaves. *The New phytologist*, **219**, 1156-
619 1169.
- 620 Dixon HH, Joly J (1895) On the Ascent of Sap. *Philosophical Transactions of the Royal Society*
621 *of London. B*, **186**, 563-576.
- 622 Eichert T, Goldbach HE (2008) Equivalent pore radii of hydrophilic foliar uptake routes in
623 stomatous and astomatous leaf surfaces – further evidence for a stomatal pathway.
624 *Physiologia plantarum*, **132**, 491-502.
- 625 Eller CB, Lima AL, Oliveira RS (2013) Foliar uptake of fog water and transport belowground
626 alleviates drought effects in the cloud forest tree species, *Drimys brasiliensis*
627 (Winteraceae). *The New phytologist*, **199**, 151-162.

- 628 Eller CB, Lima AL, Oliveira RS (2016) Cloud forest trees with higher foliar water uptake
629 capacity and anisohydric behavior are more vulnerable to drought and climate change.
630 *New Phytologist*, n/a-n/a.
- 631 Fernandez V, Sancho-Knapik D, Guzman P *et al.* (2014) Wettability, Polarity, and Water
632 Absorption of Holm Oak Leaves: Effect of Leaf Side and Age. *Plant Physiology*, **166**,
633 168-180.
- 634 Fisher RA, Williams M, Da Costa AL, Malhi Y, Da Costa RF, Almeida S, Meir P (2007) The
635 response of an Eastern Amazonian rain forest to drought stress: results and modelling
636 analyses from a throughfall exclusion experiment. *Global Change Biology*, **13**, 2361-
637 2378.
- 638 Fritz S, Bartholomé E, Belward A *et al.* (2003) Harmonisation , mosaicing and production of the
639 Global Land Cover 2000 database. European Commission Joint Research
640 Centre, Brussels., 41.
- 641 Fu R, Yin L, Li W *et al.* (2013) Increased dry-season length over southern Amazonia in recent
642 decades and its implication for future climate projection. *Proceedings of the National
643 Academy of Sciences of the United States of America*, **110**, 18110-18115.
- 644 Galbraith D (2010) Towards an improved understanding of climate change impacts on
645 Amazonian rainforests. Unpublished Doctor of Philosophy University of Edinburgh.
- 646 Gatti LV, Gloor M, Miller JB *et al.* (2014) Drought sensitivity of Amazonian carbon balance
647 revealed by atmospheric measurements. *Nature*, **506**, 76-80.
- 648 Gerlein-Safdi C, Koochafkan MC, Chung M, Rockwell FE, Thompson S, Caylor KK (2018) Dew
649 deposition suppresses transpiration and carbon uptake in leaves. *Agricultural and Forest
650 Meteorology*, **259**, 305-316.
- 651 Goldsmith GR (2013) Changing directions: the atmosphere–plant–soil continuum. *New
652 Phytologist*, **199**, 4-6.
- 653 Goldsmith GR, Matzke NJ, Dawson TE (2013) The incidence and implications of clouds for
654 cloud forest plant water relations. *Ecology Letters*, **16**, 307-314.
- 655 Gotsch SG, Asbjornsen H, Holwerda F, Goldsmith GR, Weintraub AE, Dawson TE (2014)
656 Foggy days and dry nights determine crown-level water balance in a seasonal tropical
657 Montane cloud forest. *Plant, cell & environment*, **37**, 261-272.
- 658 Gouvra E, Grammatikopoulos G (2003) Beneficial effects of direct foliar water uptake on shoot
659 water potential of five chasmophytes. *Canadian Journal of Botany*, **81**, 1278-1284.
- 660 Guzman-Delgado P, Earles JM, Zwieniecki MA (2018) Insight into the physiological role of
661 water absorption via the leaf surface from a rehydration kinetics perspective. *Plant Cell
662 and Environment*, **41**, 1886-1894.
- 663 Jackson RB, Canadell J, Ehleringer JR, Mooney HA, Sala OE, Schulze ED (1996) A global
664 analysis of root distributions for terrestrial biomes. *Oecologia*, **108**, 389-411.
- 665 Jupp TE, Cox PM, Rammig A, Thonicke K, Lucht W, Cramer W (2010) Development of
666 probability density functions for future South American rainfall. *New Phytologist*, **187**,
667 682-693.
- 668 Kangur O, Kupper P, Sellin A (2017) Predawn disequilibrium between soil and plant water
669 potentials in light of climate trends predicted for northern Europe. *Regional
670 Environmental Change*, **17**, 2159-2168.
- 671 Kull O, Broadmeadow M, Kruijt B, Meir P (1999) Light distribution and foliage structure in an
672 oak canopy. *Trees*, **14**, 55-64.

- 673 Le Quere C, Andres RJ, Boden T *et al.* (2013) The global carbon budget 1959-2011. *Earth*
674 *System Science Data*, **5**, 165-185.
- 675 Limm EB, Simonin KA, Bothman AG, Dawson TE (2009) Foliar water uptake: a common water
676 acquisition strategy for plants of the redwood forest. *Oecologia*, **161**, 449-459.
- 677 Mayr S, Schmid P, Laur J, Rosner S, Charra-Vaskou K, Dämon B, Hacke UG (2014) Uptake of
678 Water via Branches Helps Timberline Conifers Refill Embolized Xylem in Late Winter.
679 *Plant Physiology*, **164**, 1731-1740.
- 680 McDowell N, Pockman WT, Allen CD *et al.* (2008) Mechanisms of plant survival and mortality
681 during drought: why do some plants survive while others succumb to drought? *New*
682 *Phytologist*, **178**, 719-739.
- 683 Meir P, Wood TE, Galbraith DR, Brando PM, Da Costa ACL, Rowland L, Ferreira LV (2015)
684 Threshold Responses to Soil Moisture Deficit by Trees and Soil in Tropical Rain Forests:
685 Insights from Field Experiments. *Bioscience*, **65**, 882-892.
- 686 Meir P, Woodward I (2010) Amazonian rain forests and drought: response and vulnerability.
687 *New Phytologist*, **187**, 553-557.
- 688 Nadezhdina N, Nadezhdin V (2017) Are *Dracaena* nebulophytes able to drink atmospheric
689 water? *Environmental and Experimental Botany*, **139**, 57-66.
- 690 Nguyen HT, Meir P, Wolfe J, Mencuccini M, Ball MC (2016) Plumbing the depths: extracellular
691 water storage in specialized leaf structures and its functional expression in a three-domain
692 pressure–volume relationship. *Plant, cell & environment*, n/a-n/a.
- 693 Oliveira RS, Dawson TE, Burgess SSO (2005) Evidence for direct water absorption by the shoot
694 of the desiccation-tolerant plant *Vellozia flavicans* in the savannas of central Brazil.
695 *Journal of Tropical Ecology*, **21**, 585-588.
- 696 Oliveira RS, Eller CB, Bittencourt PR, Mulligan M (2014) The hydroclimatic and
697 ecophysiological basis of cloud forest distributions under current and projected climates.
698 *Ann Bot*, **113**, 909-920.
- 699 Pariyar S, Chang SC, Zinsmeister D, Zhou H, Grantz DA, Hunsche M, Burkhardt J (2017)
700 Xeromorphic traits help to maintain photosynthesis in the perhumid climate of a
701 Taiwanese cloud forest. *Oecologia*, **184**, 609-621.
- 702 Phillips OL, Aragao LEOC, Lewis SL *et al.* (2009) Drought Sensitivity of the Amazon
703 Rainforest. *Science*, **323**, 1344-1347.
- 704 Pisek J, Sonnentag O, Richardson AD, Möttus M (2013) Is the spherical leaf inclination angle
705 distribution a valid assumption for temperate and boreal broadleaf tree species?
706 *Agricultural and Forest Meteorology*, **169**, 186-194.
- 707 R Core Team (2015) R: A Language and Environment for Statistical Computing. pp Page,
708 Vienna, Austria, R Foundation for Statistical Computing.
- 709 Raabe K, Pisek J, Sonnentag O, Annuk K (2015) Variations of leaf inclination angle distribution
710 with height over the growing season and light exposure for eight broadleaf tree species.
711 *Agricultural and Forest Meteorology*, **214**, 2-11.
- 712 Richards LA, Fireman M (1943) Pressure-plate apparatus for measuring moisture sorption and
713 transmission by soils. *Soil Science*, **56**, 395-404.
- 714 Roderick ML (2001) On the use of thermodynamic methods to describe water relations in plants
715 and soil. *Australian Journal of Plant Physiology*, **28**, 729-742.
- 716 Rosado BHP, Holder CD (2013) The significance of leaf water repellency in ecohydrological
717 research: a review. *Ecohydrology*, **6**, 150-161.
- 718 Sack L, Holbrook NM (2006) Leaf hydraulics. *Annual review of plant biology*, **57**, 361-381.

Foliar water uptake in Amazonian trees

- 719 Scheff J, Frierson DMW (2014) Scaling Potential Evapotranspiration with Greenhouse
720 Warming. *Journal of Climate*, **27**, 1539-1558.
- 721 Schönherr J, Schmidt HW (1979) Water permeability of plant cuticles. *Planta*, **144**, 391-400.
- 722 Sherwood S, Fu Q (2014) A Drier Future? *Science*, **343**, 737-739.
- 723 Simonin KA, Santiago LS, Dawson TE (2009) Fog interception by *Sequoia sempervirens* (D.
724 Don) crowns decouples physiology from soil water deficit. *Plant, cell & environment*, **32**,
725 882-892.
- 726 Stone EC (1957) Dew as an ecological factor 2. The effect of artificial dew on the survival of
727 *Pinus-ponderosa* and associated species. *Ecology*, **38**, 414-422.
- 728 Ter Steege H, Pitman NCA, Sabatier D *et al.* (2013) Hyperdominance in the Amazonian Tree
729 Flora. *Science*, **342**, 325-+.
- 730 Tyree MT, Zimmermann MH, Tyree MT, Zimmermann MH (2002) Xylem structure and the
731 ascent of sap. In: *Xylem structure and the ascent of sap*. pp Page.
- 732 Van Genuchten MT (1980) A closed-form equation for predicting the hydraulic conductivity of
733 unsaturated soils. *Soil Science Society of America Journal*, **44**, 892-898.
- 734 Yan X, Zhou M, Dong X, Zou S, Xiao H, Ma X-F (2015) Molecular mechanisms of foliar water
735 uptake in a desert tree. *Aob Plants*, **7**.

736

737 **Tables**

738

739 **Table 1.** Description of values and distributions used in the model to quantify the effects of
 740 canopy-scale foliar water uptake.

741

Variable	Distribution	Description
Ψ_{canopy}	Normal*, mean -0.89 MPa, SD 0.5	-0.89 MPa was the mean of the predawn and midday water potentials taken in dry season 2015 and wet season 2014. The range between predawn and midday water potentials were around 1 MPa in both seasons.
k	Uniform, range 0 to 3.8	A mean value for k ($\text{mg m}^{-2} \text{MPa}^{-1} \text{s}^{-1}$) was derived using the change in water potential from wetting experiments and capacitance measured from pressure-volume curves. The range of K represents the interquartile range, while the mean was $2.2 \text{ mg m}^{-2} \text{Mpa}^{-1} \text{s}^{-1}$.
L	Normal, mean 5.5, SD 1	Mean and range of leaf area index consistent with previous estimates. The value 5.5 is equivalent to 50% of the entire leaf surface area being wet, i.e., one side of all leaves being wet.
P_p	Normal*, mean 0.47, SD 0.05	The proportion of time leaves are wet. Value is a mean of the annual values taken from 15 years of meteorological data. Leaf wetness duration = $D_d + D_r + N\bar{D}_e$ where is D_d duration of dew events, D_r the duration of precipitation events, N the number of precipitation events, and \bar{D}_e is the mean length of time for canopy drying following a rain event.

742 Normal* is a 'truncated normal' distribution, i.e., a normally distributed population of values
 743 from which impossible values have been removed e.g. values < 0 or > 1 , as appropriate for a
 744 proportion. SD = standard deviation.

745

746

747

748 **Figure Captions**

749 **Figure 1.** Water potentials of detached leaves collected at midday before and after being exposed
750 to experimental 'rain' for one hour. Water potential is significantly less negative in post-rain
751 leaves ($P < 0.001$, one-tailed, paired Wilcoxon test).

752

753 **Figure 2.** The change in leaf water potential (Ψ) versus initial water potential of leaves which
754 were separately exposed to: a) one hour of artificial rainfall; and b) 16 hours in a high humidity
755 atmosphere ($> 98\%$ RH) resulting in condensation on the leaves.

756

757 **Figure 3.** The water potential of leaves collected at midday and submerged in water for 3
758 minute intervals, with the petiole remaining out of the water ($n = 72$). The regression line shows
759 a non-linear fit of the form $\Psi_{\text{leaf}} = \Psi_{\text{initial}} e^{-t/RC}$, where t is the rehydration time and RC is a fitted
760 parameter equivalent to the time constant ($P < 0.001$, residual standard error = 0.4461). This
761 equation is consistent with rehydration according to a charging capacitor (Brodrribb & Holbrook,
762 2003) and assumes the final Ψ_{leaf} will tend towards 0 MPa; if the final Ψ_{leaf} is assumed to tend
763 towards a non-zero negative value, the residual error is marginally smaller at 0.4284, $P < 0.001$.

764

765 **Figure 4.** The relationship between predawn leaf water potential (Ψ_{predawn}) and sample height.
766 Data points in the white area are above the maximum theoretical Ψ values ($\Psi_{t_{\text{max}}}$) considering
767 tree height only (and no soil moisture deficit). The points in the grey area are above the $\Psi_{t_{\text{max}}}$
768 considering both tree height and soil water potential. Mean soil water potential at depths 0.5 and
769 1.0 m, at 05:00 hrs, over the course of the measurements, from 8 – 12/12/2016, was -2.19 MPa
770 meaning that all of the leaf water potentials had less negative Ψ values (ie were 'wetter') than
771 the soil to that depth. Symbols represent genera whereby the closed circles, squares and triangles
772 are *Eschweilera*, *Licania* and *Swartzia*, respectively; and the open circles, squares and triangles
773 are *Manilkara*, *Pouteria* and *Protium*, respectively. The genus-level replication is insufficient to
774 determine if the difference between genera represented by closed and open symbols is
775 significant. Each point represents a mean leaf water potential per tree from a minimum of 3

776 leaves per tree +/- standard error; one outlying point (*Pouteria*, 2.55 MPa) was removed for the
777 sake of clarity, but was included in the calculation of the mean value.

778

779 **Figure 5.** Distribution of predawn leaf water potentials in the dry and wet season. All leaves
780 were taken from a height of >15 m above the ground. All points above the dashed horizontal line
781 (=25/99 points in total, 25% of all data) are higher (i.e. 'wetter') than the theoretical maximum
782 possible leaf water potential, after accounting for the height of the leaves, and making the
783 assumption that the soil water potential is always 0 MPa. Each point from which the box plots
784 are derived represents the mean water potential of at least two leaves per tree per field campaign,
785 dry season $n = 60$, wet season $n = 39$; one outlying point (*Pouteria*, 2.55 MPa) was removed for
786 the sake of clarity.

787

788 **Figure 6.** The difference between mean leaf predawn and soil water potential ($\Psi_{\text{predawn}} - \Psi_{\text{soil}}$).
789 All points which are above 0, the horizontal dashed line, represent leaves with a water potential
790 higher (less negative, or 'wetter') than the soil. The seasonal difference is significant at $P <$
791 0.001. Each point from which the box plots are derived represents the mean water potential of at
792 least two leaves per tree per field campaign, dry season $n = 38$, wet season $n = 43$.

793

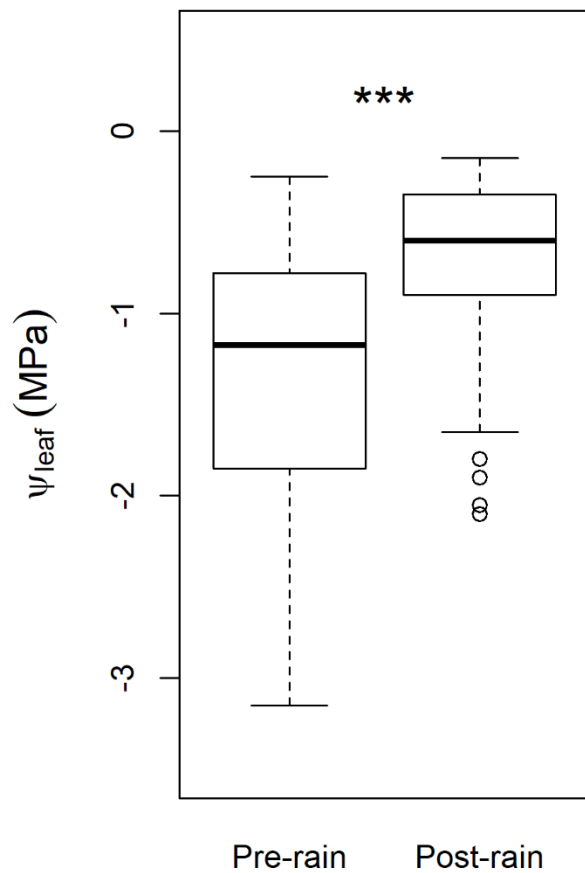
794 **Figure 7.** Probability distribution of the contribution of foliar water uptake to a) the total
795 amount of water taken up annually by the forest canopy at Caxiuanã and b), the percent of annual
796 transpiration. The bold vertical line indicates the median of the distribution of modelled outputs;
797 the box indicates the first and third quartile; the lower whisker represents the lower range of the
798 data while the upper whisker shows 1.5 times the interquartile range.

799

800

802 **Figures**

803

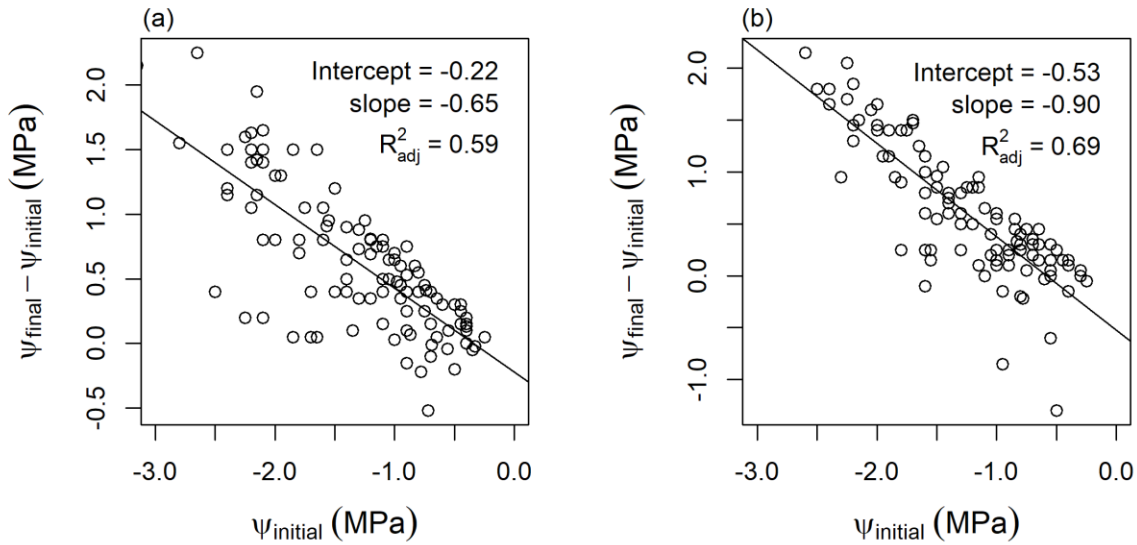


804

805 **Figure 1.** Water potentials of detached leaves collected at midday before and after being exposed

806 to experimental 'rain' for one hour. Water potential is significantly less negative in post-rain

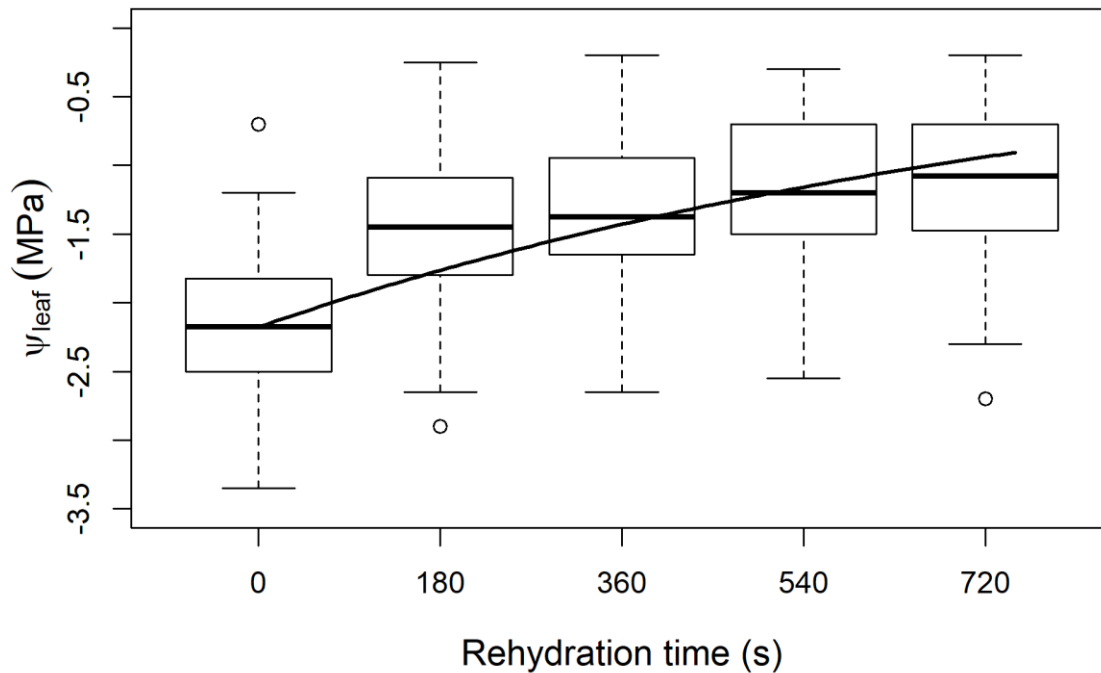
807 leaves ($P < 0.001$, one-tailed, paired Wilcoxon test).



808

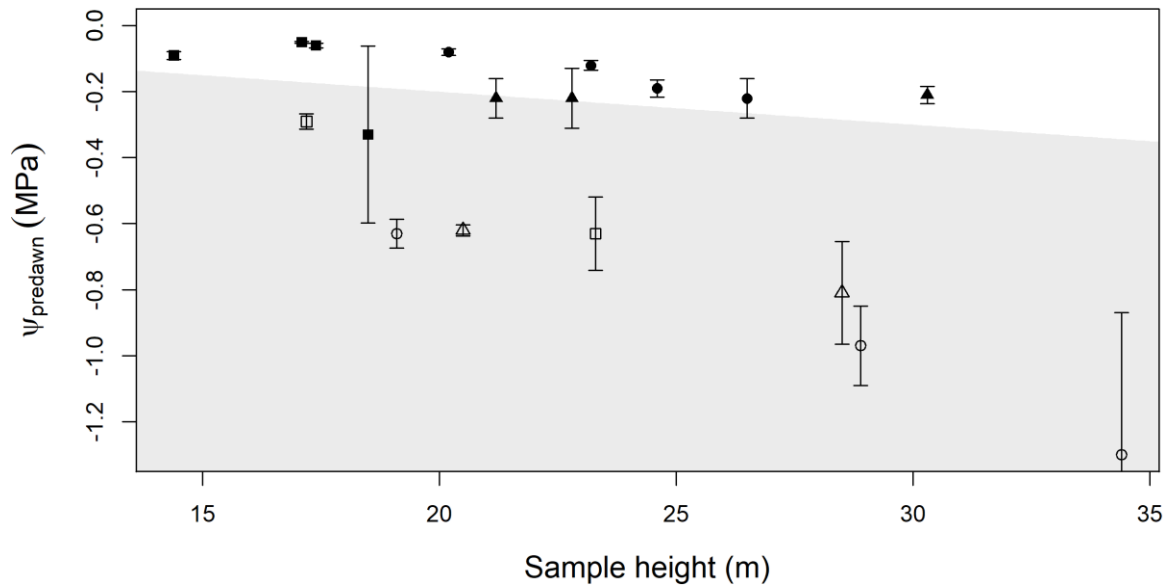
809 **Figure 2. The change in leaf water potential (Ψ) versus initial water potential of leaves**
810 **which were separately exposed to: a) one hour of artificial rainfall; and b) 16 hours in a**
811 **high humidity atmosphere (> 98 % RH) resulting in condensation on the leaves.**

812



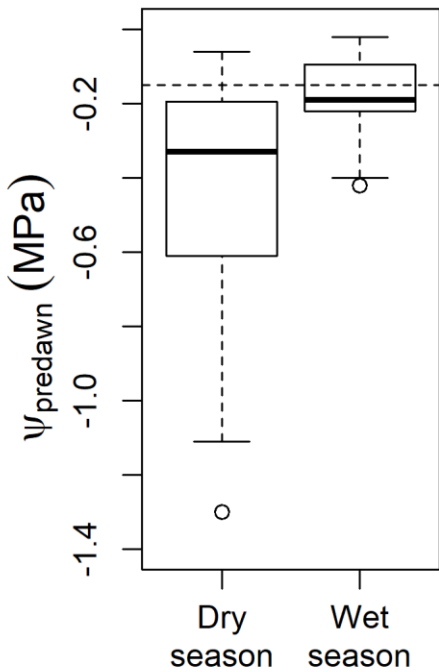
813

814 **Figure 3.** The water potential of leaves collected at midday and submerged in water for 3
815 minute intervals, with the petiole remaining out of the water ($n = 72$). The regression line
816 shows a non-linear fit of the form $\Psi_{\text{leaf}} = \Psi_{\text{initial}} e^{-t/RC}$, where t is the rehydration time and
817 RC is a fitted parameter equivalent to the time constant ($P < 0.001$, residual standard error
818 = 0.4461). This equation is consistent with rehydration according to a charging capacitor
819 (Brodribb & Holbrook, 2003) and assumes the final Ψ_{leaf} will tend towards 0 MPa; if the
820 final Ψ_{leaf} is assumed to tend towards a non-zero negative value, the residual error is
821 marginally smaller at 0.4284, $P < 0.001$.



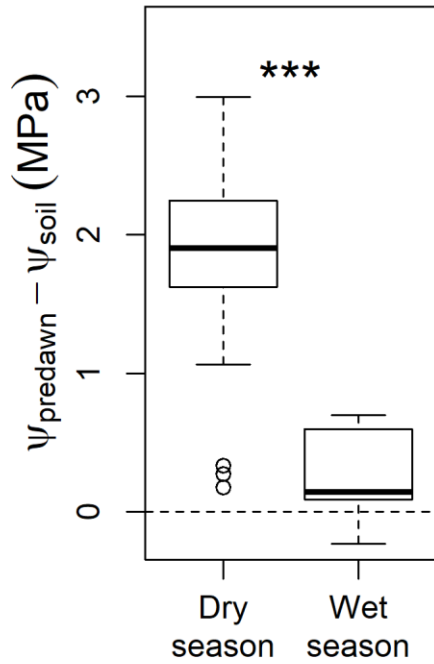
822

823 **Figure 4.** The relationship between predawn leaf water potential (Ψ_{predawn}) and sample
 824 height. Data points in the white area are above the maximum theoretical Ψ values (Ψ_{t_max})
 825 considering tree height only (and no soil moisture deficit). The points in the grey area are
 826 above the Ψ_{t_max} considering both tree height and soil water potential. Mean soil water
 827 potential at depths 0.5 and 1.0 m, at 05:00 hrs, over the course of the measurements, from 8
 828 – 12/12/2016, was -2.19 MPa meaning that all of the leaf water potentials had less negative
 829 Ψ values (ie were ‘wetter’) than the soil to that depth. Symbols represent genera whereby
 830 the closed circles, squares and triangles are *Eschweilera*, *Licania* and *Swartzia*, respectively;
 831 and the open circles, squares and triangles are *Manilkara*, *Pouteria* and *Protium*,
 832 respectively. The genus-level replication is insufficient to determine if the difference
 833 between genera represented by closed and open symbols is significant. Each point
 834 represents a mean leaf water potential per tree from a minimum of 3 leaves per tree +/-
 835 standard error; one outlying point (*Pouteria*, 2.55 MPa) was removed for the sake of
 836 clarity, but was included in the calculation of the mean value.



837

838 **Figure 5.** Distribution of predawn leaf water potentials in the dry and wet season. All leaves
839 were taken from a height of >15 m above the ground. All points above the dashed horizontal line
840 (=25/99 points in total, 25% of all data) are higher (i.e. 'wetter') than the theoretical maximum
841 possible leaf water potential, after accounting for the height of the leaves, and making the
842 assumption that the soil water potential is always 0 MPa. Each point from which the box plots
843 are derived represents the mean water potential of at least two leaves per tree per field campaign,
844 dry season $n = 60$, wet season $n = 39$; one outlying point (*Pouteria*, 2.55 MPa) was removed for
845 the sake of clarity.

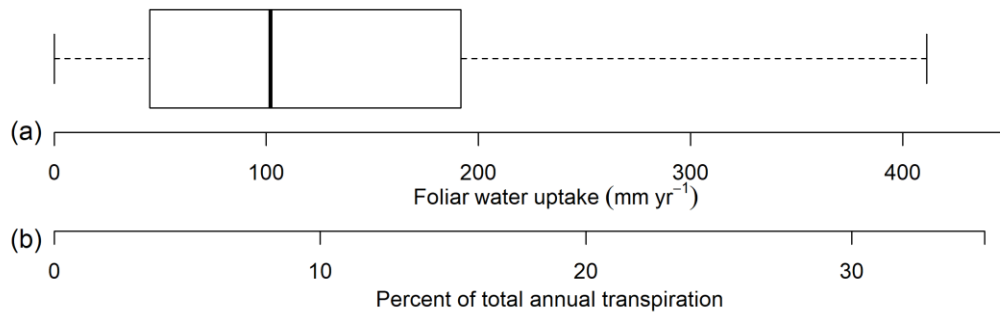


846

847 **Figure 6. The difference between mean leaf predawn and soil water potential ($\Psi_{\text{predawn}} -$**
848 **Ψ_{soil}). All points which are above 0, the horizontal dashed line, represent leaves with a**
849 **water potential higher (less negative, or ‘wetter’) than the soil. The seasonal difference is**
850 **significant at $P < 0.001$. Each point from which the box plots are derived represents the**
851 **mean water potential of at least two leaves per tree per field campaign, dry season $n = 38$,**
852 **wet season $n = 43$.**

853

Foliar water uptake in Amazonian trees



854

855 **Figure 7. Probability distribution of the contribution of foliar water uptake to a) the total**
856 **amount of water taken up annually by the forest canopy at Caxiuanã and b), the percent of**
857 **annual transpiration. The bold vertical line indicates the median of the distribution of**
858 **modelled outputs; the box indicates the first and third quartile; the lower whisker**
859 **represents the lower range of the data while the upper whisker shows 1.5 times the**
860 **interquartile range.**

861

862